"LIGHTING UP" NMR AND MRI IN COLLOIDAL AND INTERFACIAL SYSTEMS

A. PINES, J.W. LOGAN, M.M. SPENCE
Materials Sciences Division, Lawrence Berkeley National Laboratory, and Department of Chemistry, University of California at Berkeley, Berkeley, CA 94720 USA

1. ABSTRACT

By means of optical pumping with laser light, the nuclear spin polarization of gaseous xenon can be enhanced by many orders of magnitude. The enhanced polarization has allowed an extension of the pioneering experiments of Fraissard and coworkers to novel applications of NMR and MRI in chemistry, materials science and biomedicine. Examples are presented of developments and applications of laser-polarized xenon NMR and MRI on distance scales from nanometers to meters. The size of the xenon atom is similar to that of small organic molecules, such as methane, yet the nuclear magnetic resonance (NMR) signal from xenon proves a more sensitive probe for the local environment. Laser-polarized xenon NMR has been used, in collaboration with Sozzani and coworkers, to investigate the interactions present in an effectively one-dimensional gas phase inside nanochannels. Small changes in channel size and/or structure lead to very different modes of diffusion. Optically pumped Xe NMR can distinguish between these different diffusion modes out to unparalleled time scales (several tens of seconds). These studies are particularly useful for gaining a fundamental understanding of the laws that govern heterogenous mass transport such as gas transport into porous catalysts or molecular sieves, or liquid transport through pore-forming transmembrane proteins in biological systems. The understanding of mass transport inside microporous materials is crucial for many industrial and commercial processes. Recent experiments will also be described in which xenon has been used to investigate the cavities of biological nanosystems and in which polarization has been transferred to molecules on surfaces and in solution. As an example, in collaboration with Wemmer and coworkers, xenon has been used as a molecular probe to investigate the hydrophobic surfaces and interiors of macrocyclic molecules and proteins; recent results show evidence for binding of xenon to the outside of a protein, a proposed cause of the anesthetic mechanism of xenon. Indeed, localized injection of polarized xenon solutions into human blood has provided observations of the real-time process of xenon penetrating red blood cells. The injection technique also makes it possible to provide enhanced magnetic resonance images of localized areas in living organisms. Furthermore, the use of laser-polarized xenon also opens an exciting new frontier in the possibility of "functionalized xenon" as a biosensor of analytes and metabolites in

J. Fraissard and O. Lapina (eds.), Magnetic Resonance in Colloid and Interface Science, 97–106.

chemistry, materials science and biomedicine. The novel biosensor offers advantages of multiplexing capabilities and the possibility of detection in-vivo.

2. FIGURES

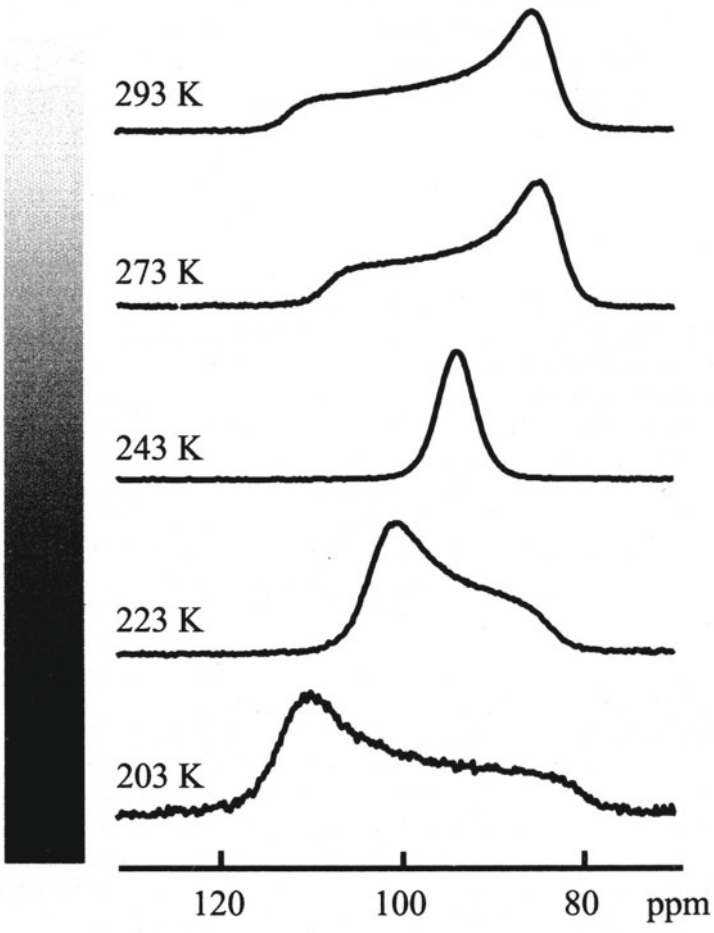

Figure 1. ^{129}Xe line shapes for xenon gas inside one-dimensional channels of Tris(*o*-phenylenedioxy)cyclotriphosphazene (TPP) at different temperatures. Although the xenon is in the gas phase, the interactions of xenon with the channel wall or other xenon atoms in the same channel distort the xenon chemical shift anisotropy (CSA) tensor, resulting in an orientation dependent chemical shift. Increasing the density of xenon in the channels, either by lowering the temperature, or increasing the mole fraction in the gas mixture (data not shown for the latter case), induces a change in the sign of the (CSA). The progression from an oblate to a prolate symmetry of the CSA is smooth, passing through a region where the line shape is isotropic. The line shapes indicate the xenon atom have cylindrical symmetry imposed upon them from the interplay of the xenon atoms with the walls of the channels (forces perpendicular to the channel axis) and the adjacent xenon atoms in the channels (forces parallel to the channel axis). Figure adapted with permission from reference 16.

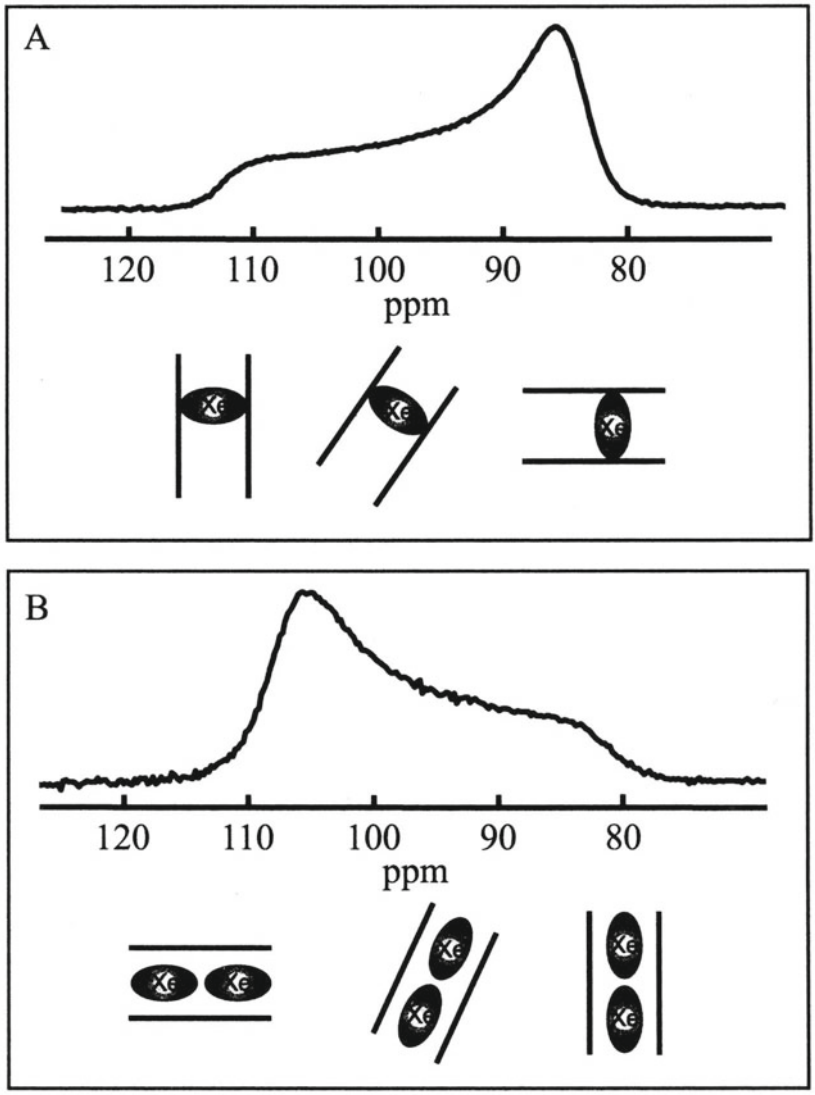

Figure 2. (A) At high temperatures or low pressures of xenon in the channels, the xenon atoms will be far apart from one another. Under these circumstances, the bonding interaction between the xenon atom and the π-electrons in the walls of the channels yield a CSA tensor with an effective oblate symmetry, resulting in a positive CSA. (B) At low temperatures or high pressures, the xenon atoms will be close to each other. In this case, the xenon–xenon Van der Waals interaction dominates the bonding interactions with the walls, and yielding a prolate symmetry in the CSA tensor and a negative CSA value.

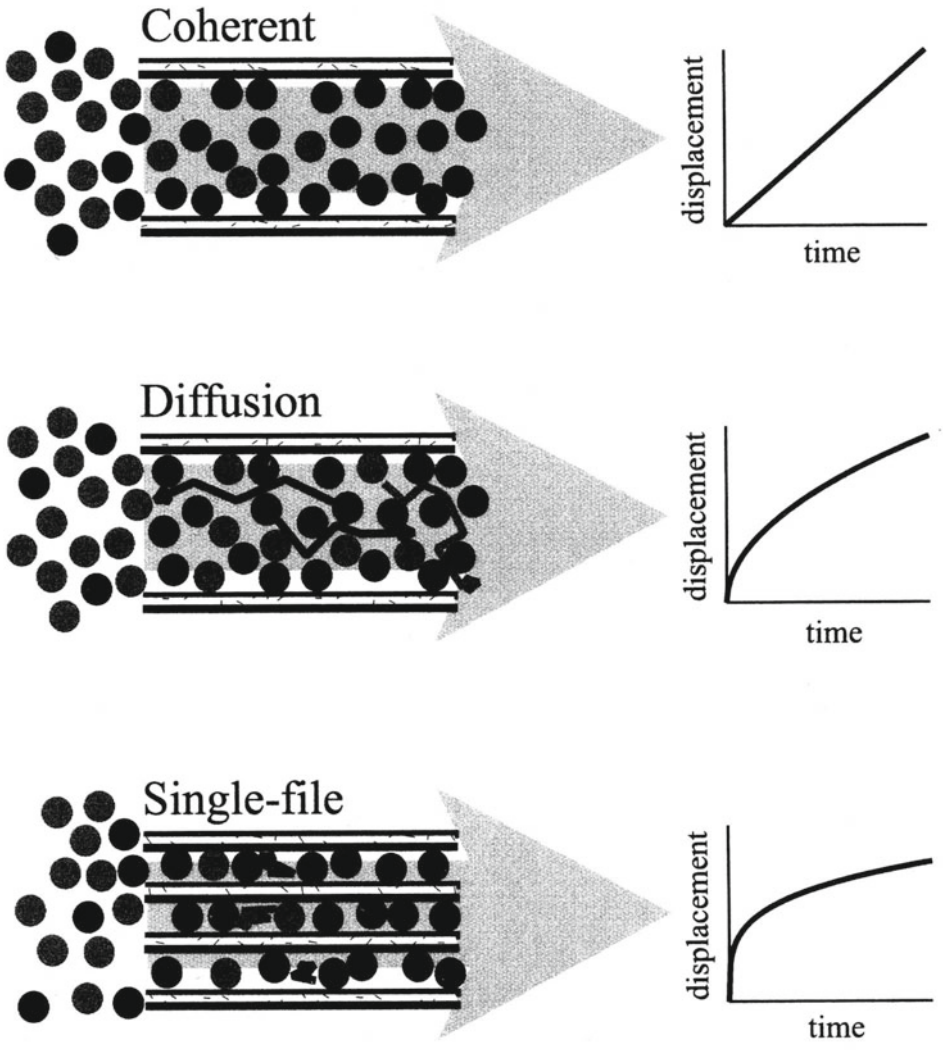

Figure 3. Gas transport caused by flow may have one of three different displacement profiles. The first is a linear displacement in time due to coherent motion (top). The second involves displacement that scales as the square root of time due to [normal] diffusion (even in the case of unidirectional diffusion) (middle). The last case is single-file diffusion (bottom). Single-file diffusion has a displacement proportional to the fourth root of time (for short times). The slower displacement is due to the inability of the atoms to "jump over", or switch places, with adjacent atoms. In small channels, such as those in TPP, single-file diffusion is observed. Figure adapted with permission from reference 6.

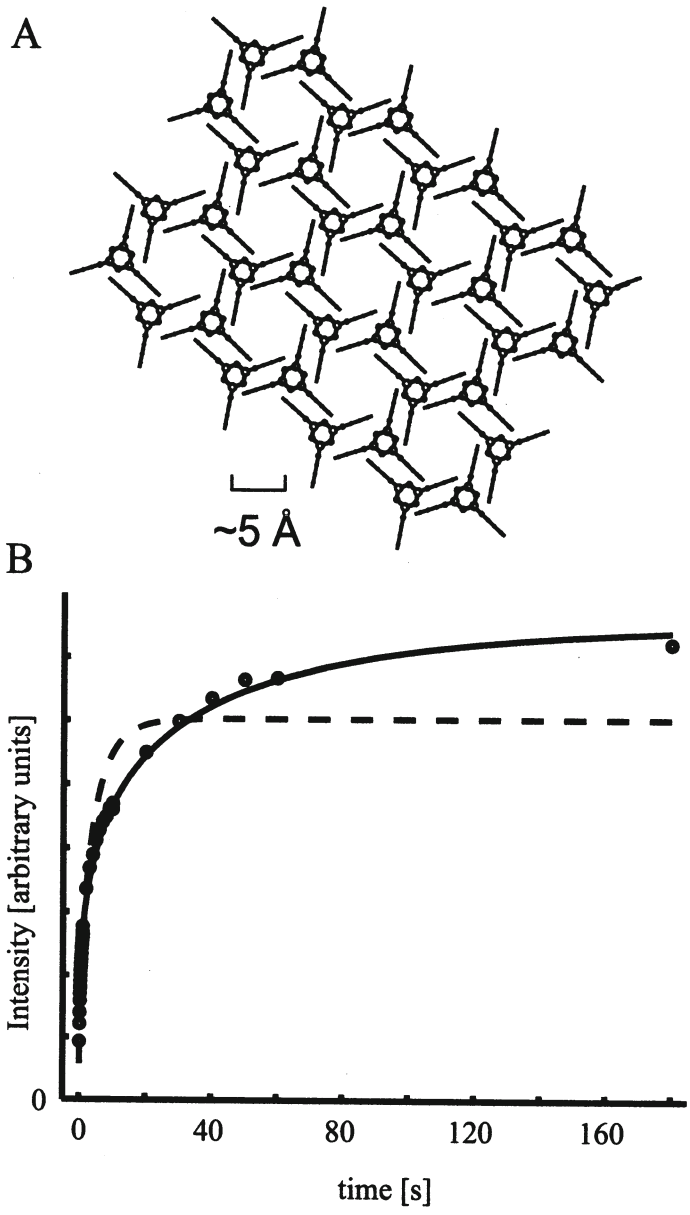

Figure 4. (A) The structure of the one-dimensional nanochannels in TPP (top view). (B) The circles indicate the intensity of the xenon resonance from the xenon gas inside the TPP channels as a function of build-up time. The solid line is a nonlinear least-squares regression of the data to a single-file diffusion model. The dashed line is the nonlinear least-squares regression of the data to a normal diffusion model. It is clear that the xenon atoms inside the TPP channels exhibit single-file diffusion behavior. Prior to the start of the build-up period, a series of $\pi/2$ saturation pulses were applied to the sample to destroy all of the xenon polarization. Next, optically polarized xenon gas flows into the sample and begins to diffuse into the TPP channels. The signal intensity as a function of build-up time increases for short times, and then levels off, as the rate of polarized xenon entering the channels equals the rate of polarization loss due to relaxation in the channels. The methods used in this work allow one to determine the mode of diffusion up to tens of seconds, whereas conventional pulsed-field gradient methods can only be used up to ~1 s. Figure adapted with permission from reference 6.

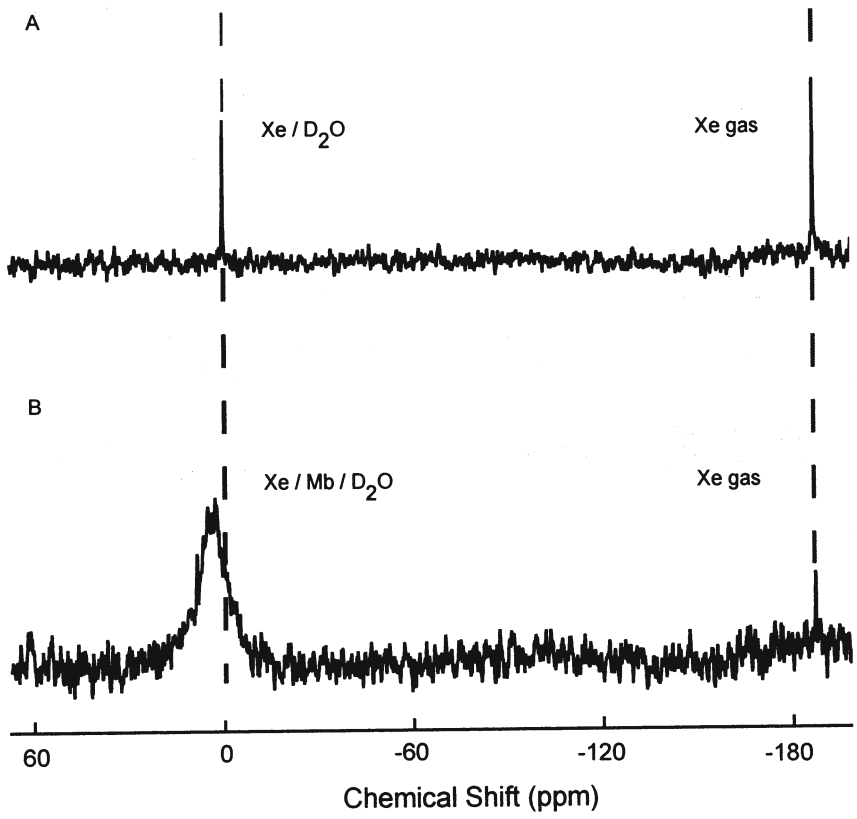

Figure 5. Typical ^{129}Xe NMR spectra of thermally polarized xenon gas dissolved (A) D_2O and (B) a 10 mM metmyoglobin solution under ~5 atm of xenon overpressure are shown. The upfield peak corresponds to xenon gas filling a capillary tube placed within the samples for *in situ* referencing. The addition of protein both shifts and significantly broadens the dissolved xenon resonance, indicating fast exchange between protein and solvent environments. Xenon has been shown to bind to small hydrophobic pockets ubiquitous in proteins, and has been used as a probe of these internal binding sites. Figure adapted with permission from reference 12.

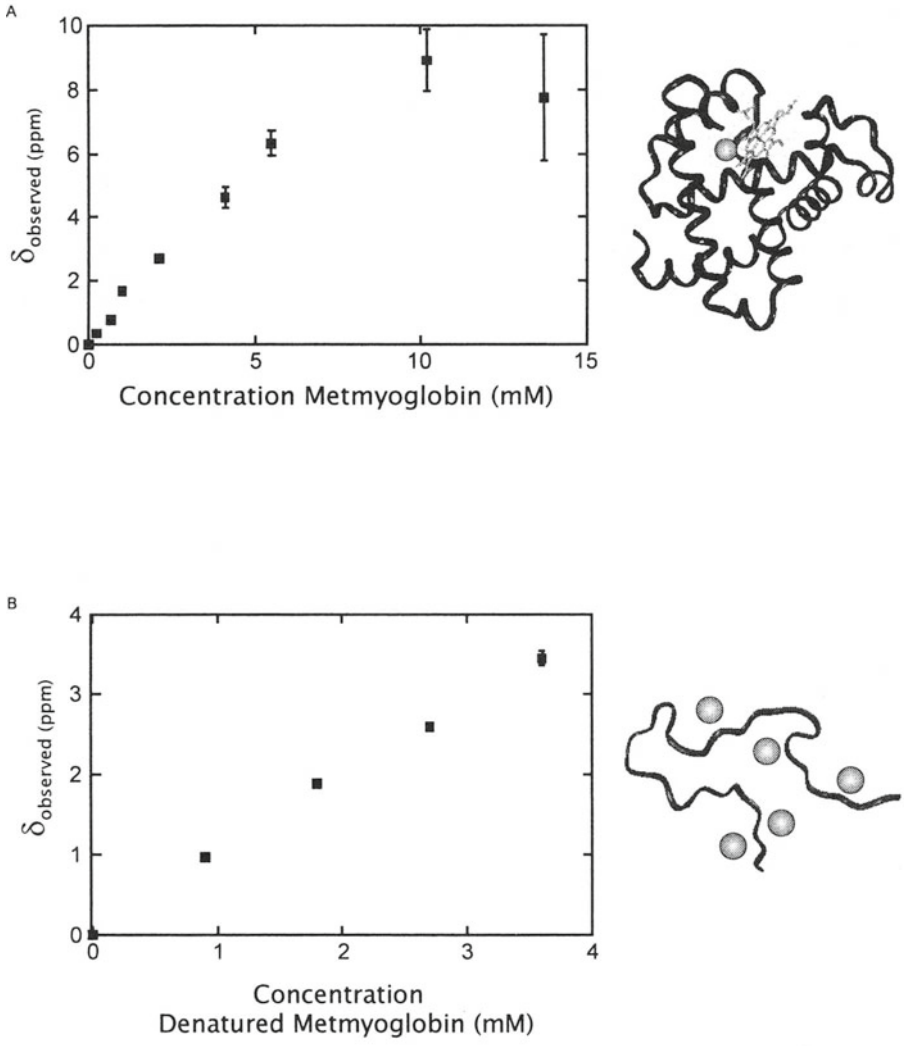

Figure 6. Both specific and non-specific interactions between xenon and myoglobin are noted. To observe the effect of myoglobin on the xenon chemical shift, the xenon resonance is measured in a series of solutions of varying protein concentration (A). The chemical shift moves downfield from that in water with increasing protein concentration but seems to have an upfield component that becomes significant at higher concentrations. The initial downfield shift reflects non-specific surface interactions between free xenon and the myoglobin. The upfield component appears as more protein is added and more xenon samples the internal binding site. In denatured myoglobin, the specific binding site is removed and only non-specific interactions exist. The titration of denatured myoglobin (B) shows a linear downfield trend over the accessible protein concentrations. Figure adapted with permission from reference 12.

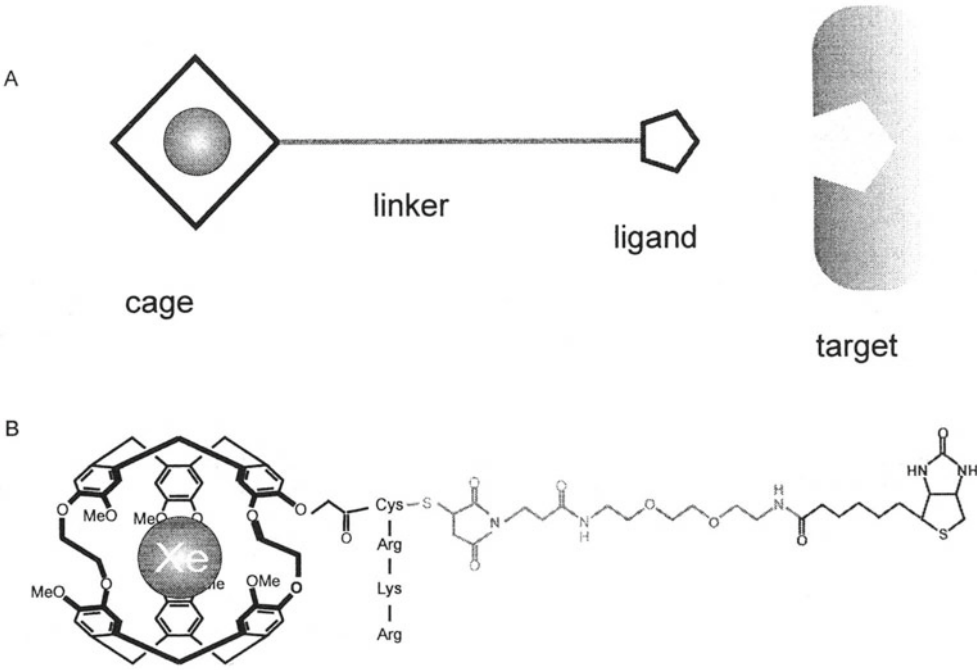

Figure 7. To make xenon detect only specific binding events, rather than all xenon-protein interactions in the solution, xenon must be targeted to a particular protein by functionalizing the xenon. This is accomplished by trapping xenon in a cage and using a linker to connect the xenon cage to a ligand that binds strongly to the target. As a prototype biosensor, a water-soluble cryptophane-A cage was attached to biotin via a linker. Biotin is a small vitamin which binds to the protein avidin with one of the largest protein-ligand binding constants known ($K \sim 10^{15}\ M^{-1}$). Figure adapted with permission from reference 17.

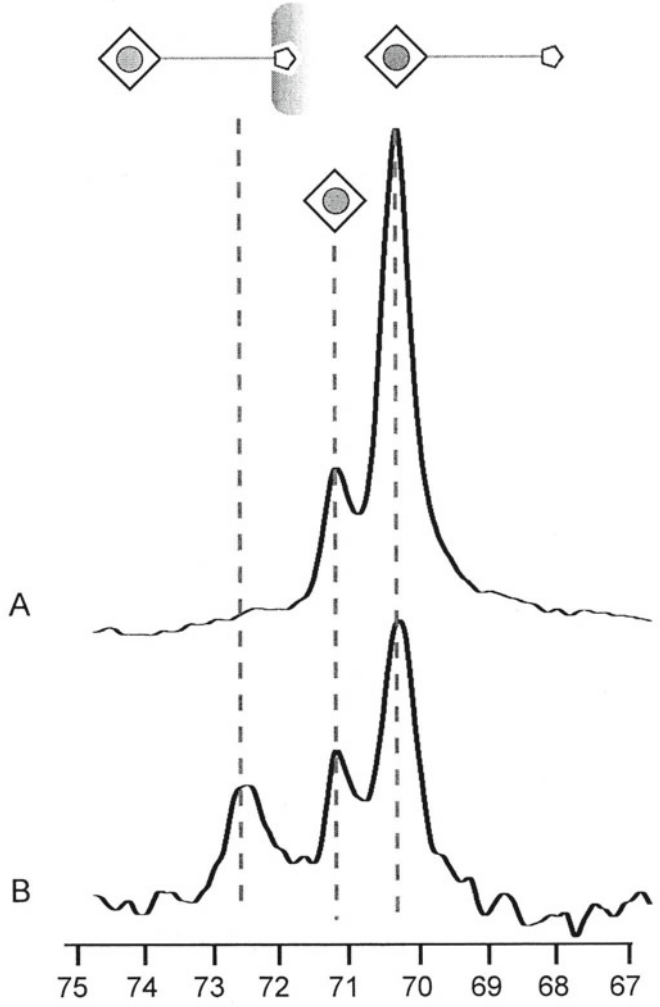

Figure 8. Spectrum A shows the functionalized xenon without avidin, with the more intense peak corresponding to functionalized xenon and the smaller peak corresponding to xenon in the bare cage, serving as both a chemical shift and signal intensity reference. Spectrum B shows the spectrum upon the addition of ~80 nmol of avidin monomer. A third peak, corresponding to functionalized xenon bound to avidin, has appeared and the unbound functionalized xenon peak has decreased in intensity. Figure adapted with permission from reference 17.

3. References

1. Albert, M. S., Cates, G. D., Driehuys, B., Happer, W., Saam, B., Springer, C. S. and Wishnia, A. (1994) Biological Magnetic Resonance Imaging using laser polarized Xe-129, *Nature*, **370**, 199-201.
2. Eckenhoff, R.G. and Johansson, J.S. (1997) Molecular interactions between inhaled anesthetics and proteins, *Pharmacol. Rev.*, **49**, 343-367.
3. Fraissard, J. and Ito, T. (1988) ^{129}Xe N.M.R. study of adsorbed xenon: A new method for studying zeolites and metal-zeolites, *Zeolites*, **76**, 350-361.
4. Hahn, K., Kärger J., and Kukla, V. (1996) Single-file diffusion observation, *Phys. Rev. Lett.*, **76**, 2762-2765.
5. Kärger J., Petzold, M., Pfeifer, H., Ernst, S., and Weitekamp, J. (1992) Single-file Diffusion and reaction in Zeolites, *J. Catal.*, **136**, 283-299.
6. Meersmann, T., Logan, J.W., Simonutti, R, Caldarelli, S., Comotti, A., Sozzani, P., Kaiser, L.G., and Pines, A. (2000) Exploring Single-File Diffusion in One-Dimensional Nanochannels by Laser-Polarized ^{129}Xe NMR Spectroscopy, *J. Phys. Chem. A*, 104, 11665-11670.
7. Prangé, T., Schiltz, M., Pernot, L., Colloc'h, N., Longhi, S., Bourget, W. and Fourme, R. (1998) Exploring hydrophobic binding sites in proteins with xenon or krypton. *Struct. Funct. Genet.*, **30**, 61-73.
8. Raftery, D., Long, H., Meersmann, T., Grandinetti, P.J., Reven, R., and Pines, A. (1991) High-field NMR of Adsorbed Xenon Polarized by Laser Pumping, *Phys. Rev. Lett.*, **66**, 584-587.
9. Ripmeester, J.A. (1982) Nuclear Shielding of Trapped Xenon Obtained by Proton-Enhanced, Magic-Angle Spinning Xe-129 NMR Spectroscopy, *J. Am. Chem. Soc.*, **104**, 289-290.
10. Rödenbeck, C., Kärger J., and Hahn, K. (1997) Exact analytical description of tracer exchange and particle conversion in single-file systems, *Phys. Rev. E*, **79**, 5697-5712.
11. Rubin S.M., Spence M.M., Dimitrov I.E., Ruiz E.J., Pines A., and Wemmer D.E. (2001) Detection of a conformational change in maltose binding protein by ^{129}Xe NMR. *J. Am. Chem. Soc.*, **123**, 8616-8617.
12. Rubin, S.M., Spence, M.M., Goodson, B.M., Wemmer, D.E., and Pines, A. (2000) Evidence of nonspecific surface interactions between laser-polarized xenon and myoglobin in solution. *Proc. Nat. Acad. Sci.*, **17**, 9472-9475.
13. Schoenborn, B.P., Watson, H.C. and Kendrew, J.C. (1965) Binding of xenon to sperm whale myoglobin. *Nature*, 1965, *207*, 28-30.
14. Sholl, D.S., and Lee, C.K. (2000) Influences of concerted cluster diffusion on single-file diffusion of CF_4 in $AlPO_4$-5 and Xe in $AlPO_4$-31, J.Chem. Phys., 112, 817-824.
15. Song, Y.Q., Goodson, B.M., and Pines, A. (1999) NMR and MRI using laser-polarized xenon, *Spectroscopy*, **14**, 26-33.
16. Sozzani, P., Comotti, A., Simonutti, R, Meersmann, T., Logan, J.W., and Pines, A. (2000) A Porous Crystalline Molecular Solid Explored by Hyperpolarized Xenon, *Angew. Chem. Int. Ed.*, **39**, 2695-2698.
17. Spence, M.M., Rubin, S.M., Dimitrov, I.E., Ruiz, E.J., Wemmer, D.E., Pines, A., Yao, S.Q., Feng, T., and Schultz, P.G. (2001) Functionalized xenon as a biosensor. *Proc. Nat. Acad. Sci.*, **98**, 10654-10657.